Astrophysics of gravitational wave sources

Lecture 9: Rapid population synthesis, Lidov-Kozai, cluster dynamics

Ondřej Pejcha

ÚTF MFF UK

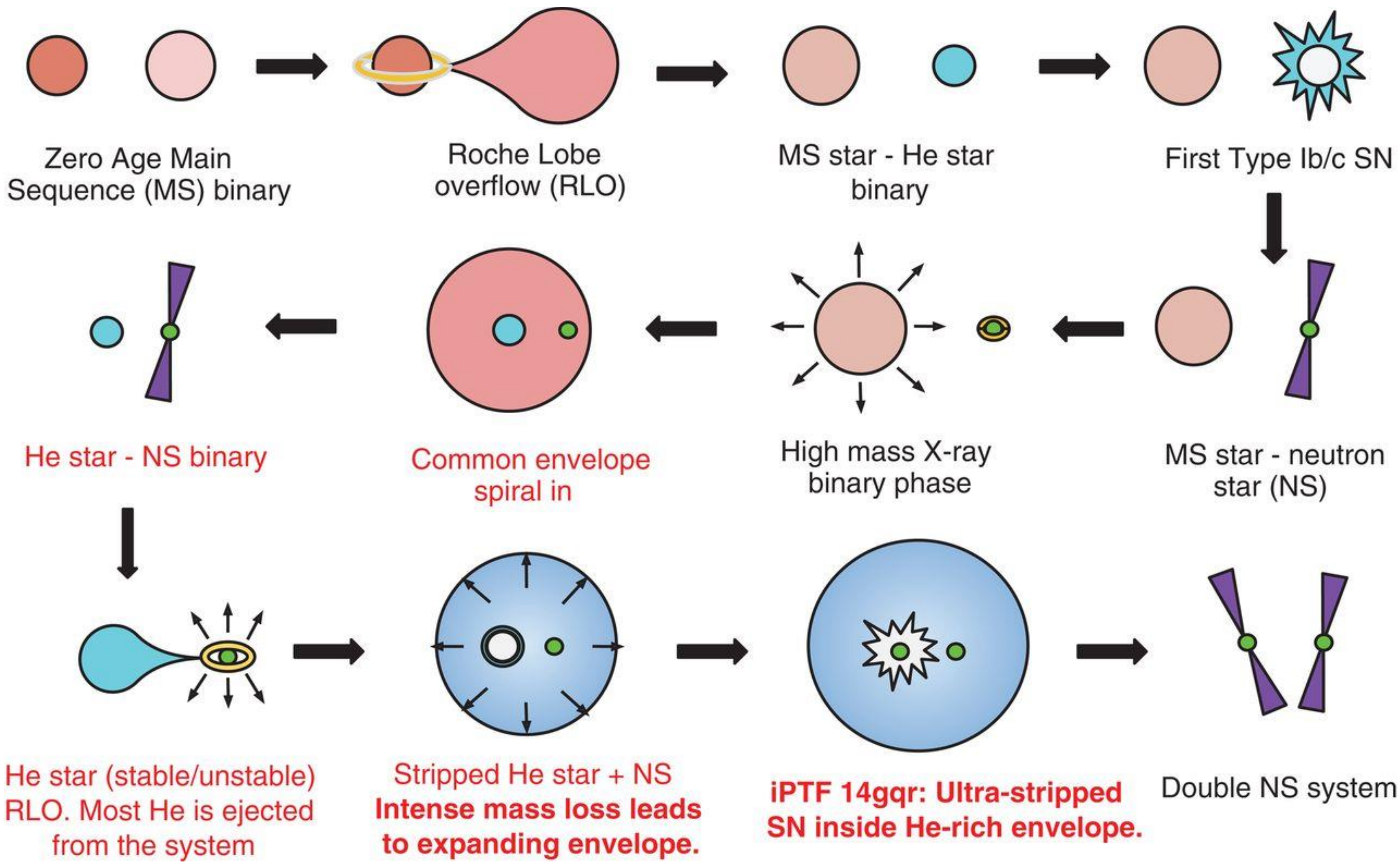

Zero Age Main Sequence (MS) binary
Roche Lobe overflow (RLO)
MS star - He star binary
First Type Ib/c SN
MS star - neutron star (NS)
High mass X-ray binary phase
Common envelope spiral in
He star - NS binary
He star (stable/unstable) RLO. Most He is ejected from the system
Stripped He star + NS
Intense mass loss leads to expanding envelope.
iPTF 14gqr: Ultra-stripped SN inside He-rich envelope.
Double NS system

De et al. (2018)

Rapid binary population synthesis

Actual single-star evolution too computationally expensive

Example based on Hurley et al. (2000)

$$\tau = \frac{t}{t_{\rm MS}} \qquad t_{\rm MS} = \frac{a_1 + a_2 M^4 + a_3 M^{5.5} + M^7}{a_4 M^2 + a_5 M^7}$$

$$\log \frac{L_{\rm MS}(t)}{L_{\rm ZAMS}} = \alpha_L \tau + \beta_L \tau^{\eta} + \left(\log \frac{L_{\rm TMS}}{L_{\rm ZAMS}} - \alpha_L - \beta_L\right)\tau^2 - \Delta L(\tau_1^2 - \tau_2^2)$$

$$L_{\rm TMS} = \frac{a_{11} M^3 + a_{12} M^4 + a_{13} M^{a_{16}+1.8}}{a_{14} + a_{15} M^5 + M^{a_{16}}}$$

$$\Delta L = \begin{cases} 0.0 & M \le M_{\rm hook} \\ B\left(\dfrac{M - M_{\rm hook}}{a_{33} - M_{\rm hook}}\right)^{0.4} & M_{\rm hook} < M < a_{33} \\ \min\left(\dfrac{a_{34}}{M^{a_{35}}}, \dfrac{a_{36}}{M^{a_{37}}}\right) & M \ge a_{33} \end{cases}$$

$$\alpha_L = \begin{cases} a_{49} & M < 0.5 \\ a_{49} + 5.0(0.3 - a_{49})(M - 0.5) & 0.5 \le M < 0.7 \\ 0.3 + (a_{50} - 0.3)(M - 0.7)/(a_{52} - 0.7) & 0.7 \le M < a_{52} \\ a_{50} + (a_{51} - a_{50})(M - a_{52})/(a_{53} - a_{52}) & a_{52} \le M < a_{53} \\ a_{51} + (B - a_{51})(M - a_{53})/(2.0 - a_{53}) & a_{53} \le M < 2.0, \end{cases}$$

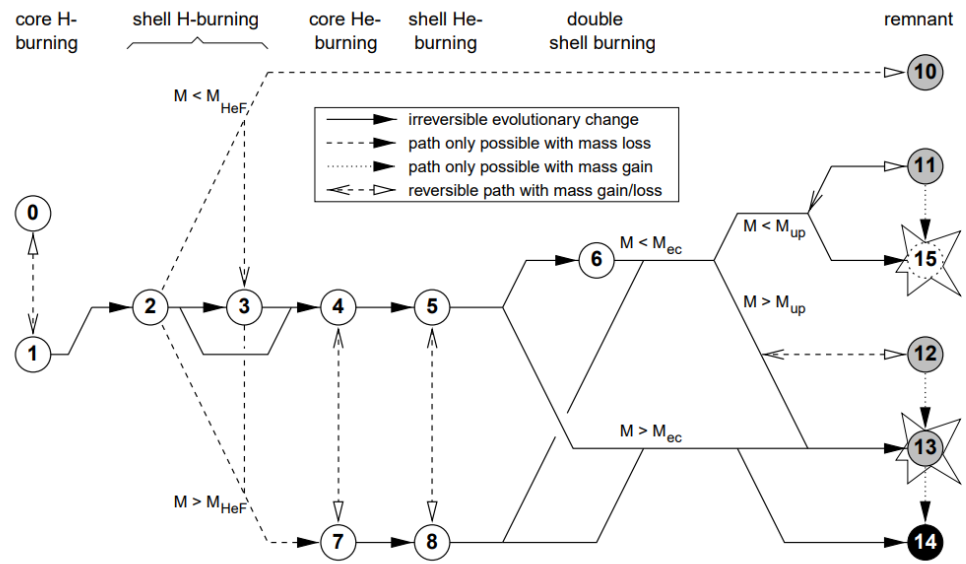

0 = main sequence M < 0.7 $M_\odot$
1 = main sequence M > 0.7 $M_\odot$
2 = Herstzsprung gap / subgiant
3 = first-ascent red giant
4 = horizontal branch / helium-burning giant
5 = early asymptotic giant / red supergiant
6 = thermally pulsating asymptotic giant
7 = naked helium main sequence
8 = naked helium (sub) giant
10 = helium white dwarf
11 = carbon/oxygen white dwarf
12 = oxygen/neon white dwarf
13 = neutron star
14 = black hole
15 = no stellar remnant

DOUBLE COMPACT OBJECTS. I. THE SIGNIFICANCE OF THE COMMON ENVELOPE ON MERGER RATES

the common envelope phase (a process that can affect merger rates by 2–3 orders of magnitude)

$$\alpha_{\rm CE}\left(\frac{G M_{\rm don,f} M_{\rm acc}}{2A_{\rm f}} - \frac{G M_{\rm don,i} M_{\rm acc}}{2A_{\rm i}}\right) = \frac{G M_{\rm don,i} M_{\rm don,env}}{\lambda R_{\rm don,lob}}$$

an NS/BH may form). The value of $\alpha_{\rm CE}$ has been set to 1 throughout this study. The range of values for the product $\alpha_{\rm CE}\lambda$ may therefore be covered by λ alone. The parameter λ describes

S	Standard	$\lambda =$ *Nanjing*, $M_{\rm NS,max} = 2.5\ M_\odot$, $\sigma = 265$ km s^{-1} BH kicks: variable, SN: Rapid half-cons mass transfer
V1	$\lambda = 0.01$	Very low λ: fixed
V2	$\lambda = 0.1$	Low λ: fixed
V3	$\lambda = 1$	High λ: fixed
V4	$\lambda = 10$	Very high λ: fixed

Galactic Merger Rates, $Z_\odot$ (Myr^{-1})[a]

Model	NS–NS	BH–NS	BH–BH
S	23.5 (7.6)	1.6 (0.2)	8.2 (1.9)
V1	0.4 (0.4)	0.002 (0.002)	1.1 (1.1)
V2	11.8 (1.1)	2.4 (0.08)	15.3 (0.4)
V3	48.8 (14.3)	4.6 (0.03)	5.0 (0.03)
V4	20.8 (0.3)	0.9 (0.0)	0.3 (0.0)

Dominik et al. (2012)

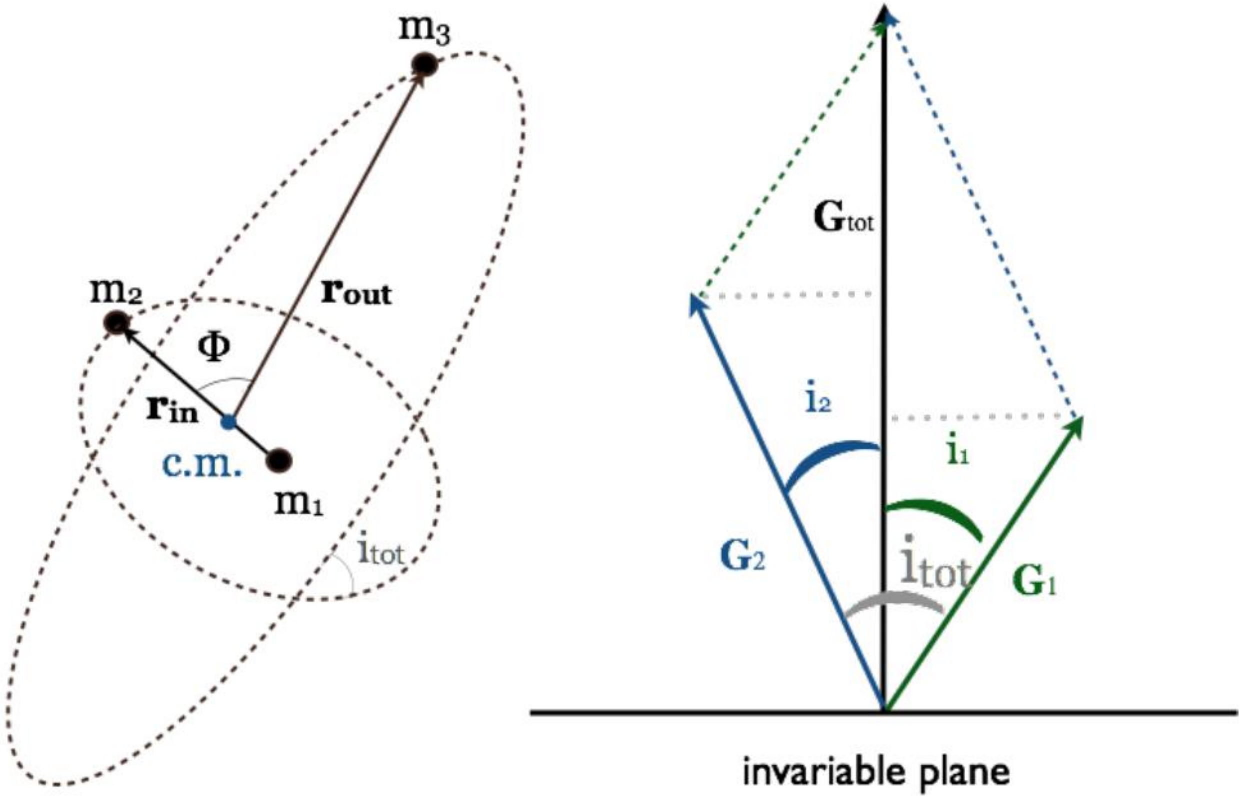

The secular approximation (i.e., phase averaged, long term evolution) can be applied, where the interactions between two non-resonant orbits is equivalent to treating the two orbits as massive wires. Here, the line-density is inversely proportional to orbital velocity and the two orbits torque each other and exchange angular momentum, but not energy. Therefore the orbits can change shape and orientation (on timescales much longer than their orbital periods), but not semi-major axes of the orbits.

Naoz (2016)

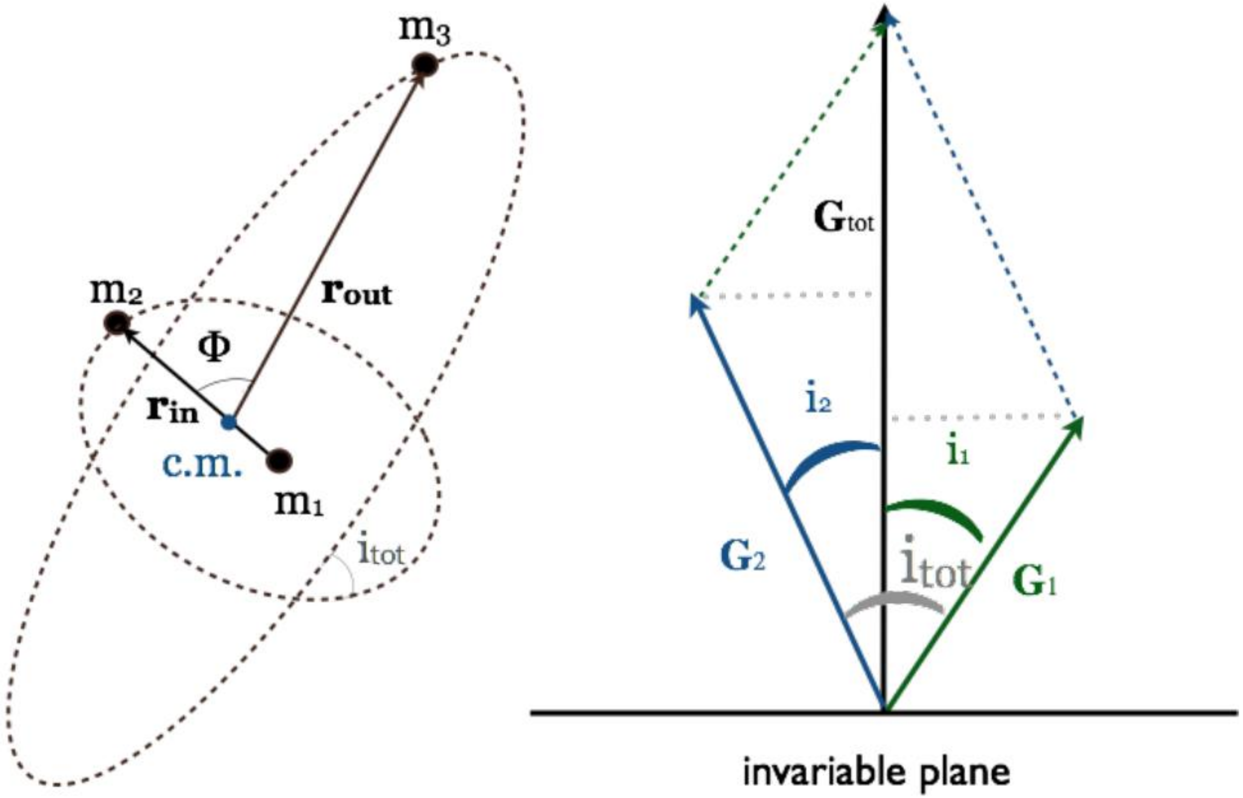

$$\mathcal{H} = \frac{k^2 m_1 m_2}{2a_1} + \frac{k^2 m_3 (m_1 + m_2)}{2a_2} + \frac{k^2}{r_2} \sum_{n=2}^{n=\infty} \left(\frac{r_{\rm in}}{r_{\rm out}}\right)^n M_n P_n(\cos\Phi)$$

$$M_n = m_1 m_2 m_3 \frac{m_1^{n-1} - (-m_2)^{n-1}}{(m_1 + m_2)^n}$$

Naoz (2016)

$$\mathcal{H} = \frac{3}{8}k^2\frac{m_1 m_3}{a_2}\left(\frac{a_1}{a_2}\right)^2\frac{1}{(1-e_2^2)^{3/2}}F_{quad}\ ,$$

$$F_{\rm quad} = -\frac{e_1^2}{2} + \theta^2 + \frac{3}{2}e_1^2\theta^2 + \frac{5}{2}e_1^2(1-\theta^2)\cos(2\omega_1)$$

$$j_{z,1} = \sqrt{1-e_1^2}\cos i_{\rm tot} = \text{Const.}$$

$$\theta = \cos i_{\rm tot}$$

arguments of periastron, ω_1 and ω_2

$$j_{z,1} = \sqrt{1-e_{1,max/min}^2}\cos i_{1,min/max} = \sqrt{1-e_{1,0}^2}\cos i_{1,0}$$

$$e_{max} = \sqrt{1-\frac{5}{3}\cos^2 i_0}$$

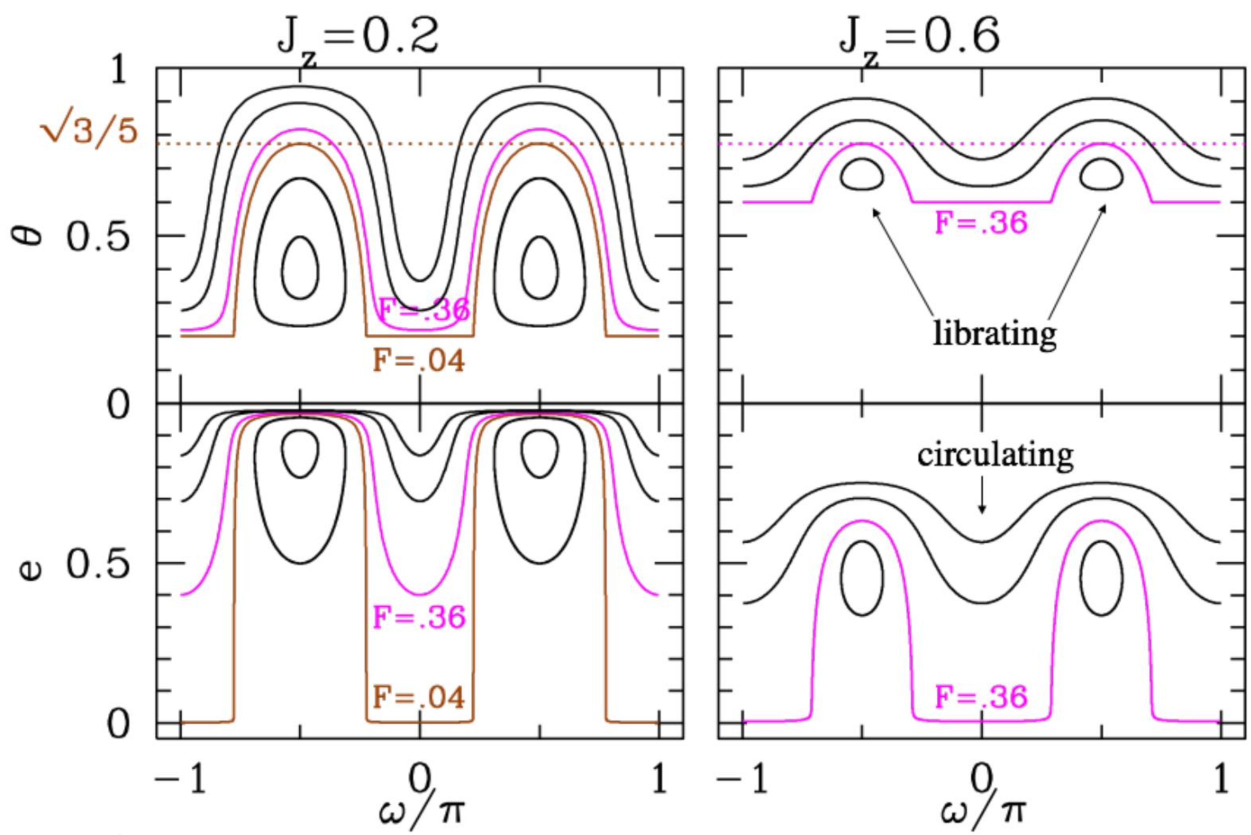

Naoz (2016)

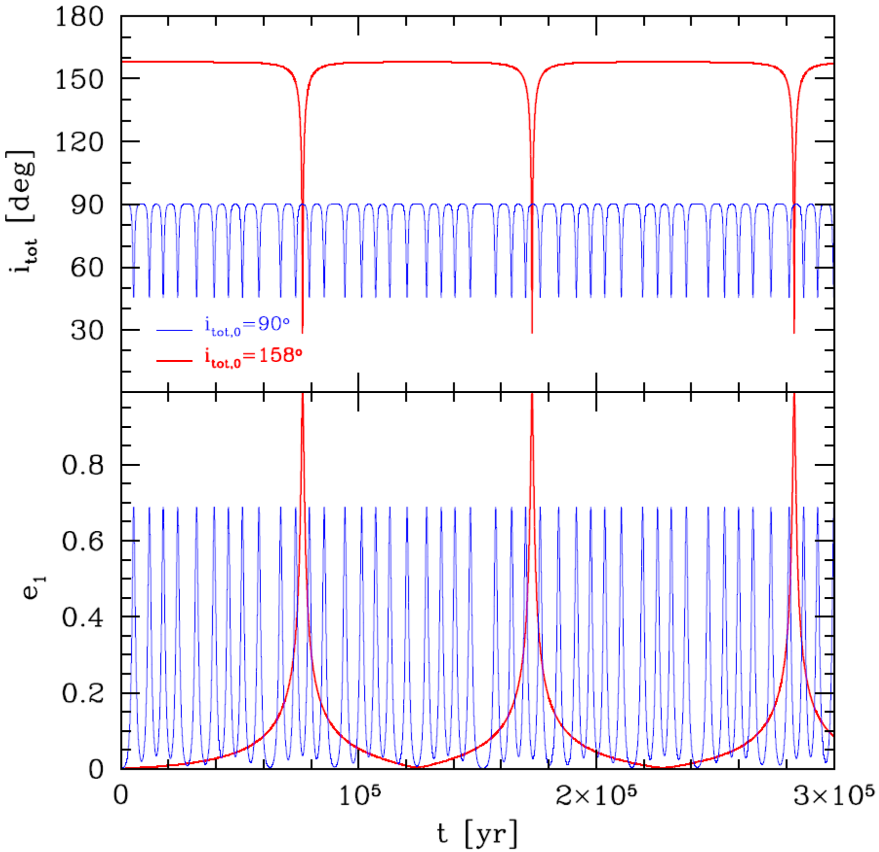

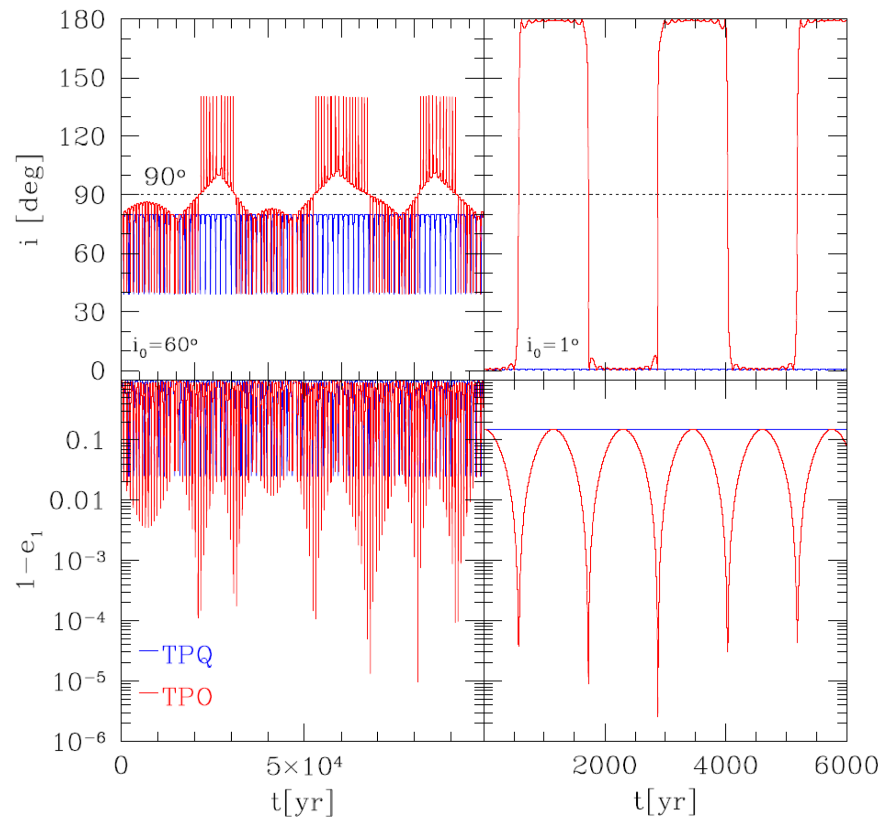

$$t_{\rm quad} \sim \frac{16}{15}\frac{a_2^3(1-e_2^2)^{3/2}\sqrt{m_1+m_2}}{a_1^{3/2}m_3 k}$$

$$= \frac{16}{30\pi}\frac{m_1+m_2+m_3}{m_3}\frac{P_2^2}{P_1}(1-e_2^2)^{3/2}$$

Naoz (2016)

Non-secular effects

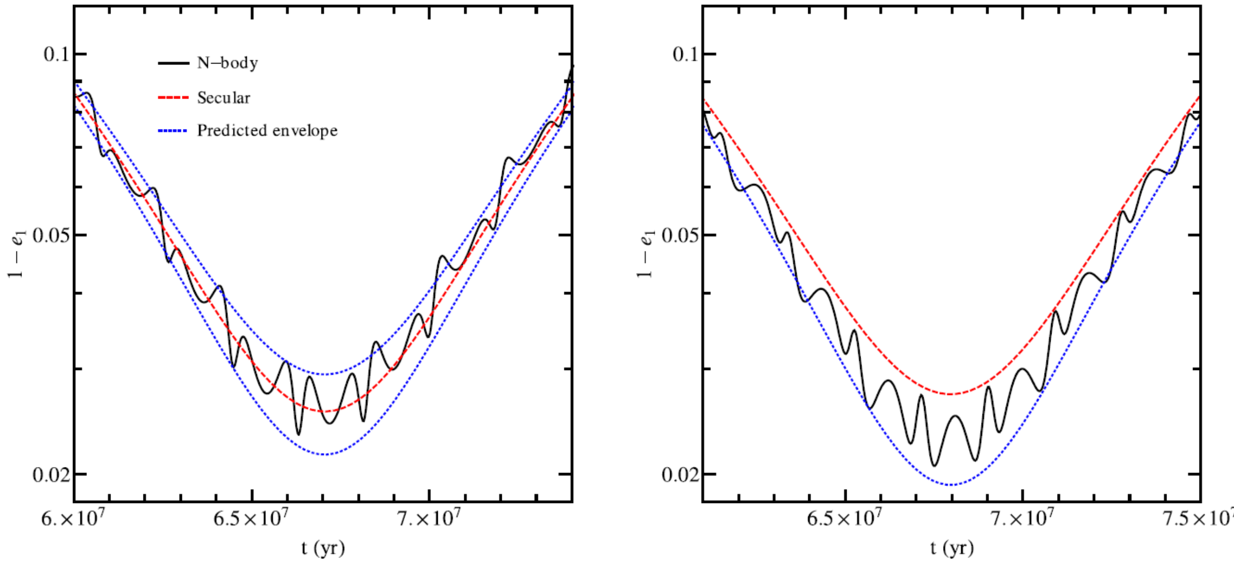

$$\left\langle \frac{da}{dt} \right\rangle = -\frac{64}{5}\frac{G^3\mu M^2}{c^5 a^3(1-e^2)^{7/2}}\left(1+\frac{73}{24}e^2+\frac{37}{96}e^4\right)$$ Antognini et al. (2014)

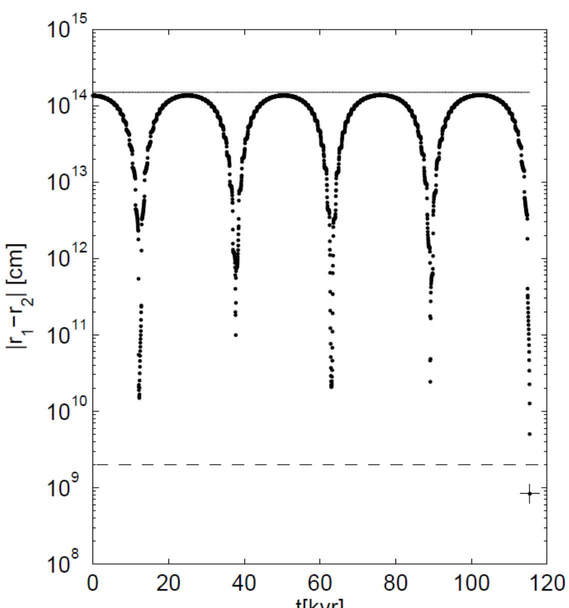

Katz & Dong (2012)

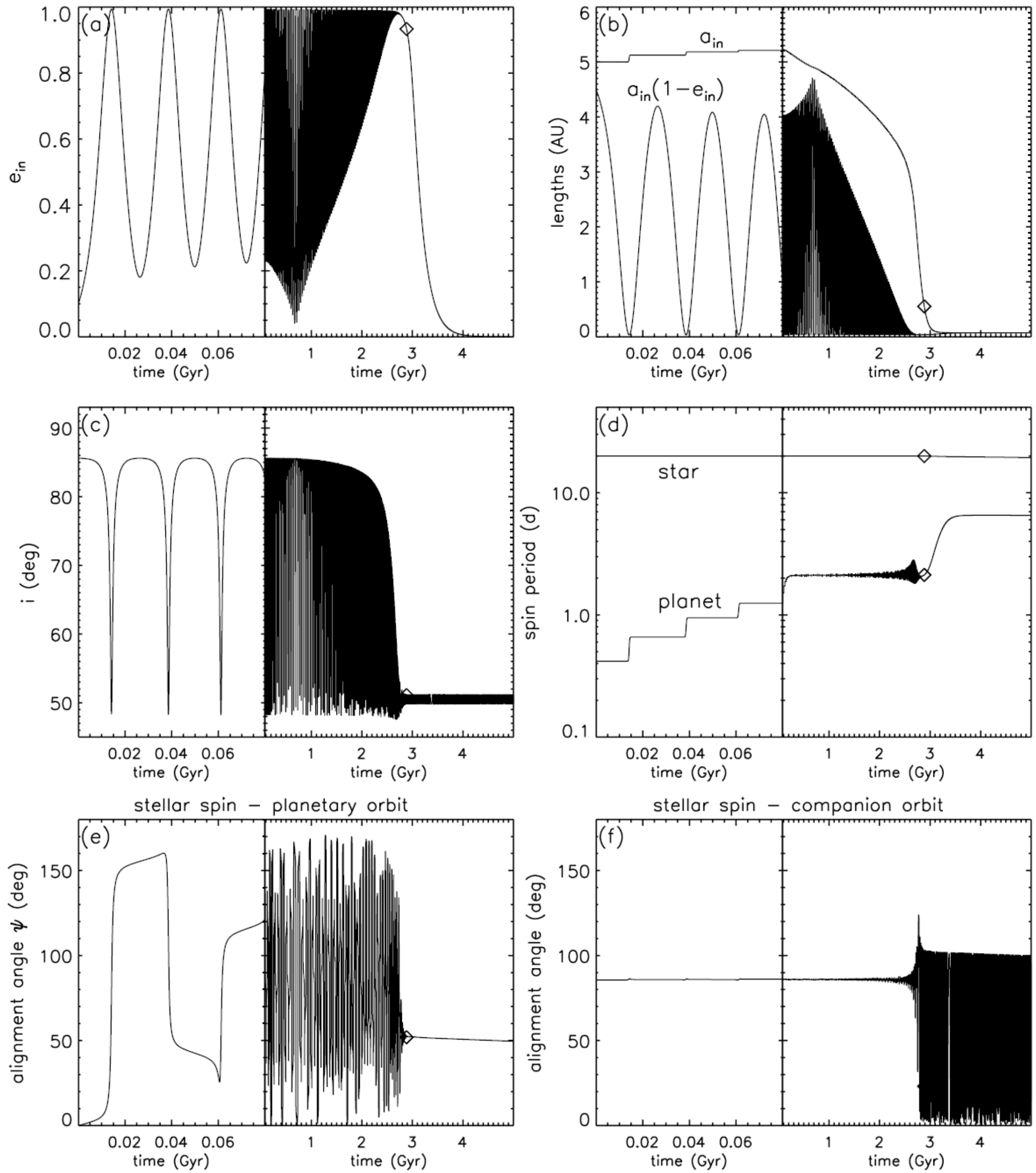

Fabrycky & Tremaine (2007)

Cluster dynamics

$$t_{\rm relax} \simeq \frac{N}{8 \ln \Lambda} t_{\rm dyn}$$

$$t_{\rm dyn} \simeq (G\bar{\rho})^{-1/2}$$

$$\ln \Lambda = \ln(b_{\rm max}/b_{\rm min})$$

$$b_{\rm min} = 2Gm/\sigma^2$$

Dehnen & Read (2011)

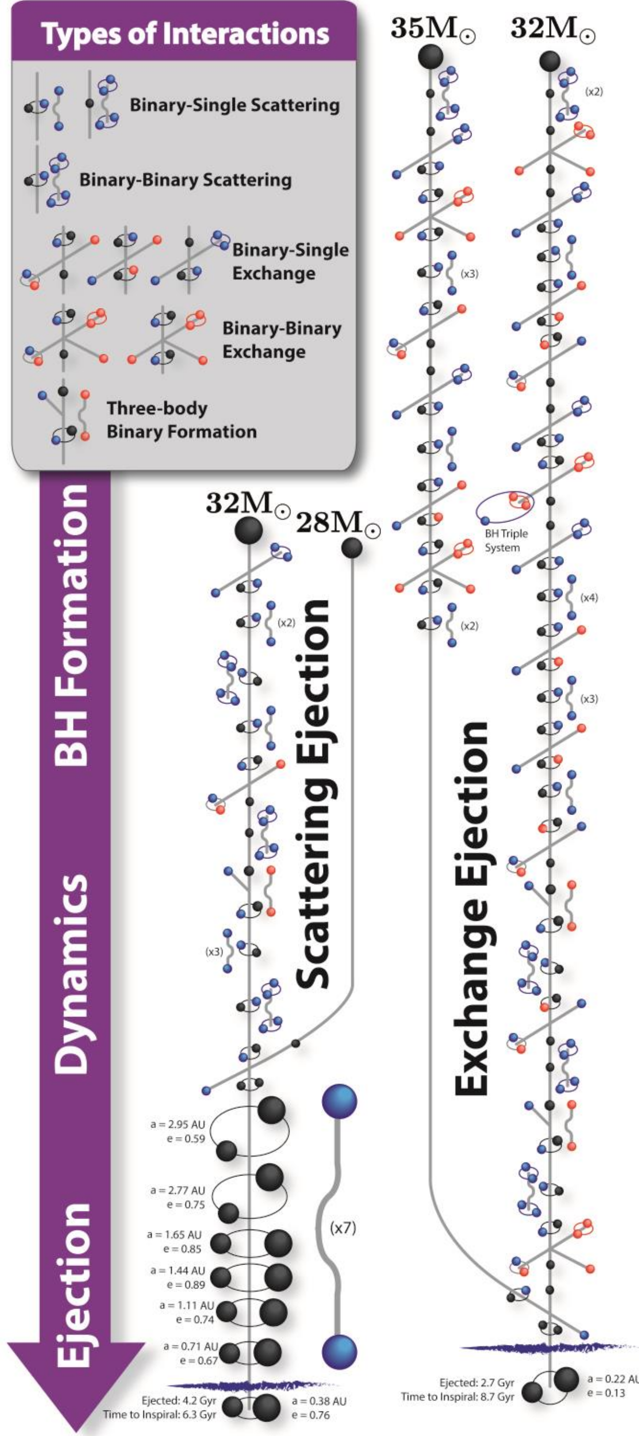

Rodriguez et al. (2016)

Cool videos

- https://www.youtube.com/watch?v=qJMom80Qdc8
- https://www.youtube.com/watch?v=3L3iSWRCtuA
- https://ciera.northwestern.edu/gallery/
- Also worth: Adler planetarium

The Double Pulsar

M. Kramer[1] and I.H. Stairs[2]

Abstract

A landmark discovery was made in 2003 when the first binary system containing two active radio pulsars was observed. Not only is this system, PSR J0737-3039A/B, the most relativistic binary system ever found, but it also exhibits eclipses and magnetospheric interactions. The observational and theoretical insights provided by this first double pulsar go far beyond applications in pulsar astrophysics alone. Timing observations of the two pulsars provide the best test of general relativity (GR) in strong gravitational fields. Studies of the system's evolution suggest the possibility of an unusual neutron star formation process. The discovery of this system has a significant impact on the expected coalescence rate of galactic double neutron stars and the detection of merging systems in Earth-bound gravitational-wave detectors. Moreover, observations and modeling of the eclipses provide evidence for relativistic spin precession and dipolar magnetic fields in pulsar magnetospheres. This paper reviews the double pulsar's properties and what they mean for fundamental physics and astrophysics.

THE MASS DISTRIBUTION OF STELLAR BLACK HOLES

CHARLES D. BAILYN[1]
Yale University, Department of Astronomy, P.O. Box 208101, New Haven, CT 06520-8101; bailyn@astro.yale.edu
RAJ K. JAIN AND PAOLO COPPI
Yale University, Department of Physics, P.O. Box 208101, New Haven, CT 06520-8101; raj.jain@yale.edu, coppi@astro.yale.edu
AND
JEROME A. OROSZ
Pennsylvania State University, Department of Astronomy, 525 Davey Laboratory, University Park, PA 16802; orosz@astro.psu.edu
Received 1997 August 5; accepted 1998 January 5

ABSTRACT

We examine the distribution of masses of black holes in transient low-mass X-ray binary systems. A Bayesian analysis suggests that it is probable that six of the seven systems with measured mass functions have black hole masses clustered near seven solar masses. There appears to be a significant gap between the masses of these systems and those of the observed neutron stars. The remaining source, V404 Cyg, has a mass significantly larger than the others, and our analysis suggests that it is probably drawn from a different distribution. Selection effects do not appear to play a role in producing the observed mass distribution, which may be explained by currently unknown details of the supernova explosions and of binary evolution prior to the supernova.

Colloquium: Measuring the neutron star equation of state using x-ray timing

Anna L. Watts

One of the primary science goals of the next generation of hard x-ray timing instruments is to determine the equation of state of matter at supranuclear densities inside neutron stars by measuring the radius of neutron stars with different masses to accuracies of a few percent. Three main techniques can be used to achieve this goal. The first involves waveform modeling. The flux observed from a hotspot on the neutron star surface offset from the rotational pole will be modulated by the star's rotation, and this periodic modulation at the spin frequency is called a pulsation. As the photons propagate through the curved spacetime of the star, information about mass and radius is encoded into the shape of the waveform (pulse profile) via special and general-relativistic effects. Using pulsations from known sources (which have hotspots that develop either during thermonuclear bursts or due to channeled accretion) it is possible to obtain tight constraints on mass and radius. The second technique involves characterizing the spin distribution of accreting neutron stars. A large collecting area enables highly sensitive searches for weak or intermittent pulsations (which yield spin) from the many accreting neutron stars whose spin rates are not yet known. The most rapidly rotating stars provide a clean constraint, since the limiting spin rate where the equatorial surface velocity is comparable to the local orbital velocity, at which mass shedding occurs, is a function of mass and radius. However, the overall spin distribution also provides a guide to the torque mechanisms in operation and the moment of inertia, both of which can depend sensitively on dense matter physics. The third technique is to search for quasiperiodic oscillations in x-ray flux associated with global seismic vibrations of magnetars (the most highly magnetized neutron stars), triggered by magnetic explosions. The vibrational frequencies depend on stellar parameters including the dense matter equation of state, and large-area x-ray timing instruments would provide much improved detection capability. An illustration is given of how these complementary x-ray timing techniques can be used to constrain the dense matter equation of state and the results that might be expected from a 10 m^2 instrument are discussed. Also discussed are how the results from such a facility would compare to other astronomical investigations of neutron star properties.

Black hole, neutron star and white dwarf candidates from microlensing with OGLE-III★

Ł. Wyrzykowski,[1]† Z. Kostrzewa-Rutkowska,[1] J. Skowron,[1] K. A. Rybicki,[1] P. Mróz,[1]

ABSTRACT

Most stellar remnants so far have been found in binary systems, where they interact with matter from their companions. Isolated neutron stars and black holes are difficult to find as they are dark, yet they are predicted to exist in our Galaxy in vast numbers. We explored the OGLE-III data base of 150 million objects observed in years 2001–2009 and found 59 microlensing events exhibiting a parallax effect due to the Earth's motion around the Sun. Combining parallax and brightness measurements from microlensing light curves with expected proper motions in the Milky Way, we identified 13 microlensing events which are consistent with having a white dwarf, neutron star or a black hole lens and we estimated their masses and distances. The most massive of our black hole candidates has 9.3 $M_\odot$ and is at a distance of 2.4 kpc. The distribution of masses of our candidates indicates a continuum in mass distribution with no mass gap between neutron stars and black holes. We also present predictions on how such events will be observed by the astrometric *Gaia* mission.